Numerical Study of an Ultrabroadband, Wide-Angle, Polarization-Insensitivity Metamaterial Absorber in the Visible Region

Nguyen Thi Quynh Hoa, Phan Duy Tung, Phan Huu Lam, Nguyen Duc Dung & Nguyen Hong Quang

Journal of Electronic Materials

ISSN 0361-5235
Volume 47
Number 5

Journal of Elec Materi (2018)
47:2634-2639
DOI 10.1007/s11664-018-6100-5

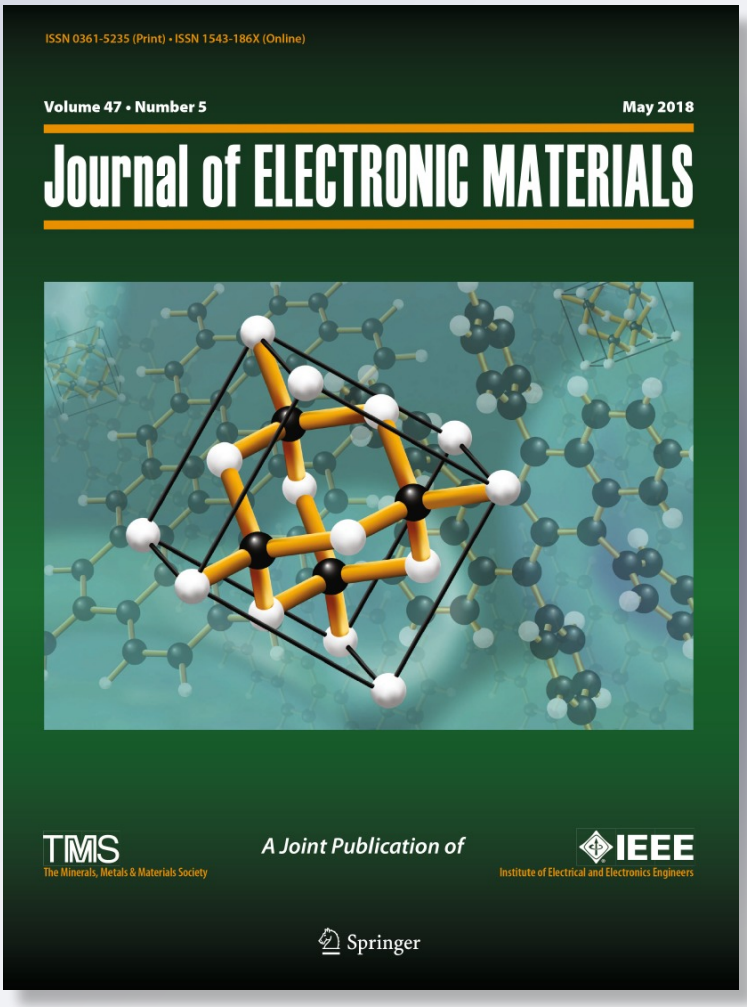

Springer

Journal of ELECTRONIC MATERIALS, Vol. 47, No. 5, 2018
https://doi.org/10.1007/s11664-018-6100-5

Numerical Study of an Ultrabroadband, Wide-Angle, Polarization-Insensitivity Metamaterial Absorber in the Visible Region

NGUYEN THI QUYNH HOA,[1,2] PHAN DUY TUNG,[1] PHAN HUU LAM,[1] NGUYEN DUC DUNG,[1] and NGUYEN HONG QUANG[1]

1.—School of Engineering and Technology, Vinh University, 182 Le Duan, Vinh City, Vietnam. 2.—e-mail: ntqhoa@vinhuni.edu.vn

We propose and numerically investigate an ultrabroadband metamaterial absorber (MA) formed of a periodic array of metallic–dielectric multilayered conical frustums for use in the visible regime. The bandwidth and absorption performance of the proposed absorber can be controlled by varying structural parameters such as the tilt angle and lattice constant. The absorption efficiency of the proposed MA exceeds 80% in a wide bandwidth from 474.4 nm to 784.4 nm and is retained at large angles of incidence up to 65°. Furthermore, perfect polarization insensitivity is also obtained due to its rotationally symmetric structure. This excellent absorber performance makes the proposed MA a promising candidate for applications in the visible region.

Key words: Metamaterials, multilayers, absorption, surface plasmons, visible frequency

INTRODUCTION

As artificial materials, metamaterials (MMs) exhibit unnatural electromagnetic properties, for instance, negative refractive index, inverse Doppler effect, etc. Such properties make them potential candidates for use in perfect lensing, electromagnetic cloaking, and perfect absorption and transmission.[1–4] Recently, metamaterial absorbers (MAs) have been studied extensively to enhance the efficiency of solar energy harvesting,[5] plasmonic sensors,[6] bolometers,[7] and wireless power transfer.[8] In particular, controllable design of MAs with wide angle of incidence and polarization insensitivity is of great interest, because electromagnetic (EM) waves can be obliquely incident onto the MA surface. Another desirable aspect of such MA design is that it allows extension of the bandwidth while maintaining high absorptivity. Use of two-dimensional patterns blending various unit cells with perfect absorber (PA) peaks[9–11] has been found to enlarge the absorption band of MAs. However, this method for extending the absorption band has disadvantages, because the number of resonances that can be blended together is limited. Recently, another approach to enhance the absorption band markedly using stacked metallic and dielectric multilayers was reported.[12–15] However, these designs are limited mainly to controlling the bandwidth by increasing the number of homogeneous layers or heterogeneous metallic and dielectric layers, which are relatively complicated and entail high cost. Furthermore, little information is available on the effect of other structural parameters on the bandwidth as well as the absorption characteristics of such MAs, including the angle of incidence and polarization.

We report herein a simple approach to design an ultrabroadband MA in the visible region using a periodic array of metallic–dielectric multilayered conical frustums. The bandwidth and absorption properties of the MA can be controlled by tuning structural parameters such as the tilt angle and lattice constant, as evaluated using numerical simulations in this work. The results reveal that the

(Received September 2, 2017; accepted January 20, 2018; published online February 5, 2018)

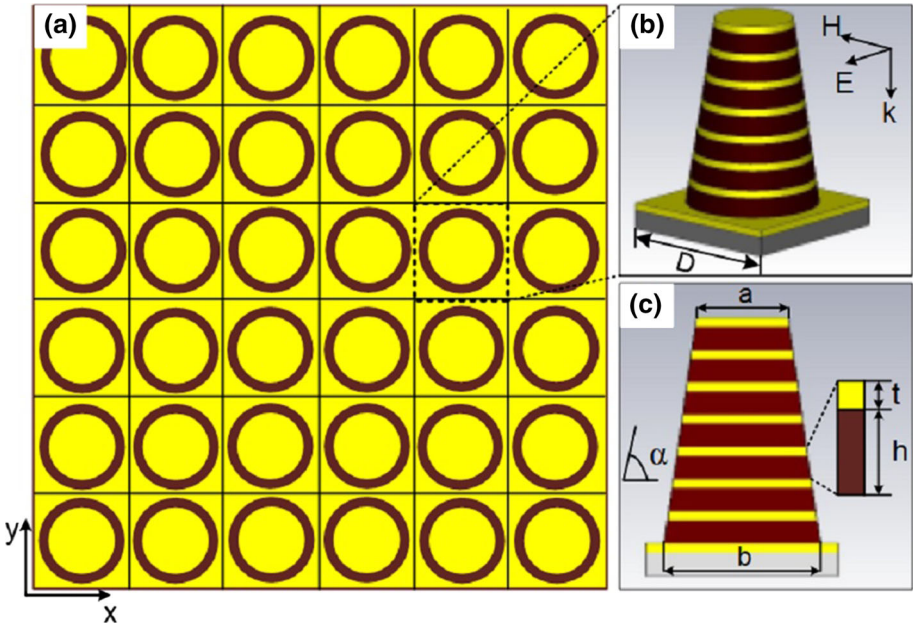

Fig. 1. Schematic of proposed MA: (a) top view, (b) three-dimensional (3-D) unit cell, and (c) central cross-section view of unit cell.

absorption properties and bandwidth of the MA depend strongly on the tilt angle, which is optimized at 88°. The MA exhibits perfect absorption across the full range of the visible region with wide angle tolerance and polarization insensitivity due to its rotationally symmetric structure. The size of the unit cell is a few tens of nanometers, which could be fabricated using current nanofabrication techniques, although this lies beyond the scope of this article.

DESIGN AND SIMULATION

Figure 1 shows a schematic diagram of the proposed ultrabroadband MA. The unit cell of the MA is a periodic array of metallic–dielectric multilayered conical frustums. The conical frustums consist of seven homogeneous metallic/dielectric pairs. A gold layer with electrical conductivity of 4.562×10^7 S/m and thickness of 15 nm and a silicon layer with relative dielectric constant of 11.9 and thickness of 60 nm are used as the metallic and dielectric layer, respectively. The base diameter (b) of the conical frustum is 65 nm. The tilt angle (α), which is created by the inclination of each lateral face with respect to the base, was varied from 85° to 89°. Meanwhile, the lateral lattice constant (D) between conical frustums was changed from 130 nm to 160 nm. On the back layer of the conical frustums, a 15-nm gold layer is used to block all transmission.

To investigate the absorption performance of the proposed MA, numerical simulations were performed using the frequency-domain solver in the computer simulation technology (CST) Microwave Studio. In the simulations, the electric and magnetic components of the EM wave are along the x and y direction, respectively, so that the wavevector $\mathbf{k}$ propagates perpendicular to the front side of the MA as depicted in Fig. 1b.

The absorption by the proposed MA was calculated as $A(\omega) = 1 - T(\omega) - R(\omega)$, where $A(\omega)$, $T(\omega)$, and $R(\omega)$ are the absorption, transmission, and reflection as a function of frequency ω, respectively. $A(\omega)$ and $T(\omega)$ were determined from the frequency-dependent S-parameter $S_{11}(\omega)$ and $S_{21}(\omega)$, where $T(\omega) = |S_{21}(\omega)|^2$ and $R(\omega) = |S_{11}(\omega)|^2$. In the conventional absorber model, the back layer acts as a physical barrier to block incident waves. Since $T(\omega)$ is eliminated by the ground plane, the absorption simplifies to $A(\omega) = 1 - |S_{11}(\omega)|^2$. The considered range of EM waves was from 400 nm to 1000 nm.

RESULTS AND DISCUSSION

The absorption spectrum and bandwidth of an MA design usually depend strongly on its structural parameters.[10,16] Figure 2 shows the absorption spectra of the proposed MA as a function of tilt angle with other structural parameters fixed, for both transverse electric (TE) and transverse magnetic (TM) polarizations. The lateral lattice constant of the proposed MA structure is 160 nm. As seen from Fig. 2, variation of the tilt angle not only affects the absorption efficiency but also influences the absorption region and bandwidth of the MA. With increasing tilt angle from 86° to 89°, the absorption spectra is red-shifted and the bandwidth reduced. This behavior can be explained by the increasing top diameter of the conical frustums. It is clear that, as the tilt angle is increased from 86° to 89°, the top diameter increases for fixed base diameter of the conical frustums. It was recently

reported that the resonant frequency is size dependent.[10] Therefore, the high resonant frequency band due to the top part is red-shifted while the low resonant frequency band due to the base part of the conical frustums is fixed, resulting in the red-shift and reduced bandwidth of the absorption spectrum. Note that high absorption efficiency above 90% is achieved across the entire visible spectrum in the range from 471.6 nm to 774.6 nm for the MA with tilt angle of 88°. To evaluate the absorption performance of the MA, we used the relative absorption bandwidth (BW), defined in Refs. 14, 17. Figure 3 shows the dependence of the BW on the tilt angle. As shown in this figure, the BW increases with increase of the tilt angle from 85° to 88°. However, the BW decreased, surprisingly, with further increase of the tilt angle up to 90°. This indicates that the highest BW value of 48.6% was achieved at tilt angle of 88°.

Beside this dependence on tilt angle, the absorption performance is also dependent on the lattice constant, as shown in Fig. 4 and summarized in Table I. The lattice constant was altered from 130 nm to 200 nm to observe the effect on the BW and the independent angle of incidence for fixed tilt angle of 88° for both the TE and TM polarizations. As shown in Fig. 4, the BW decreased with increasing lattice constant for both the TE and TM polarization. Furthermore, the proposed MA exhibits absorptivity above 90% across a bandwidth covering the visible region (480 nm to 760 nm). With lattice constant in the range from 140 nm to 170 nm, the absorption was insensitive to angle of incidence when above 50°, as indicated in Table I. For lattice constant of 150 nm, the aforementioned highest independent angle of incidence of 55° was observed for both TE and TM polarizations. The detailed absorption spectrum of the MA with lattice constant of 150 nm is shown in Fig. 5. These results show that a wide bandwidth in the range from 474.4 nm to 784.4 nm with absorptivity above 80% can be achieved and maintained for high angles of incidence up to 65°.

Furthermore, the polarization behavior of the MA was also studied under both TE and TM polarizations. Figure 6 shows the absorptivity at various

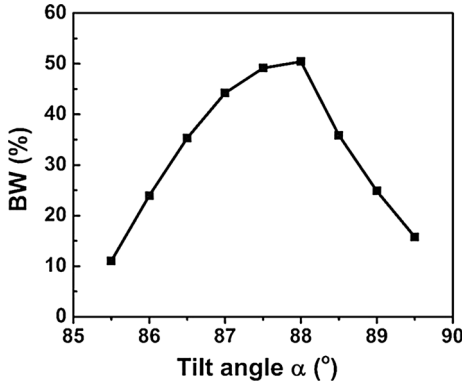

Fig. 3. Relative absorption bandwidth (BW) for various tilt angles.

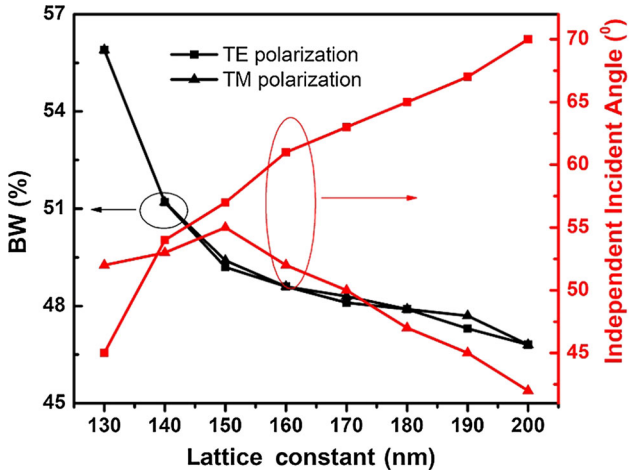

Fig. 4. Absorption of proposed MA with various lattice constants under both TE and TM polarizations.

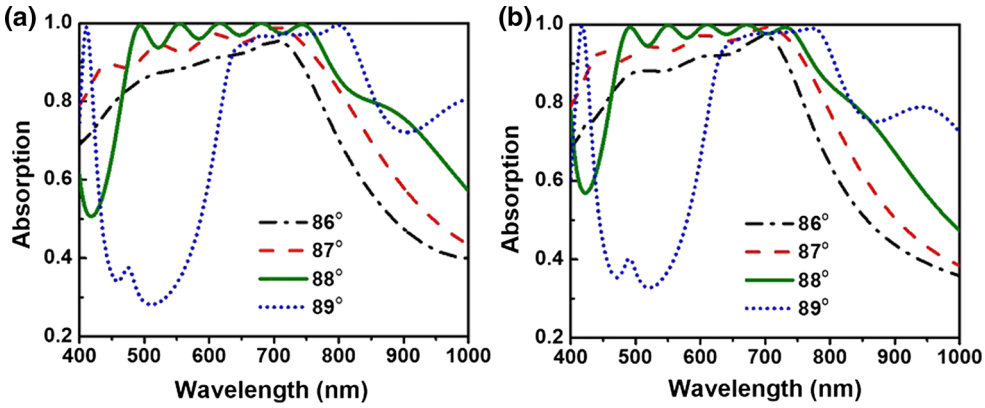

Fig. 2. Absorption spectrum of MA with various tilt angles for (a) TE and (b) TM polarization.

Table I. Absorption properties of MA designed with various lattice constants

Lattice constant (nm)	Range with > 90% absorption (nm)		Bandwidth with > 90% (%)		Independent angle with > 90% (°)	
	TE	TM	TE	TM	TE	TM
130	482.5–857.2	482.3–857.0	55.9	55.9	45	52
140	478.0–807.2	478.1–807.2	51.2	51.2	54	53
150	474.4–784.4	474.5–785.6	49.2	49.4	57	55
160	471.6–774.7	471.8–774.6	48.6	48.6	61	52
170	470.2–768.7	470.5–769.9	48.1	48.3	63	50
180	469.2–765.2	469.5–765.2	47.9	47.9	65	47
190	468.8–759.4	468.7–760.5	47.3	47.7	67	45
200	468.4–754.7	468.5–754.8	46.8	46.8	70	42

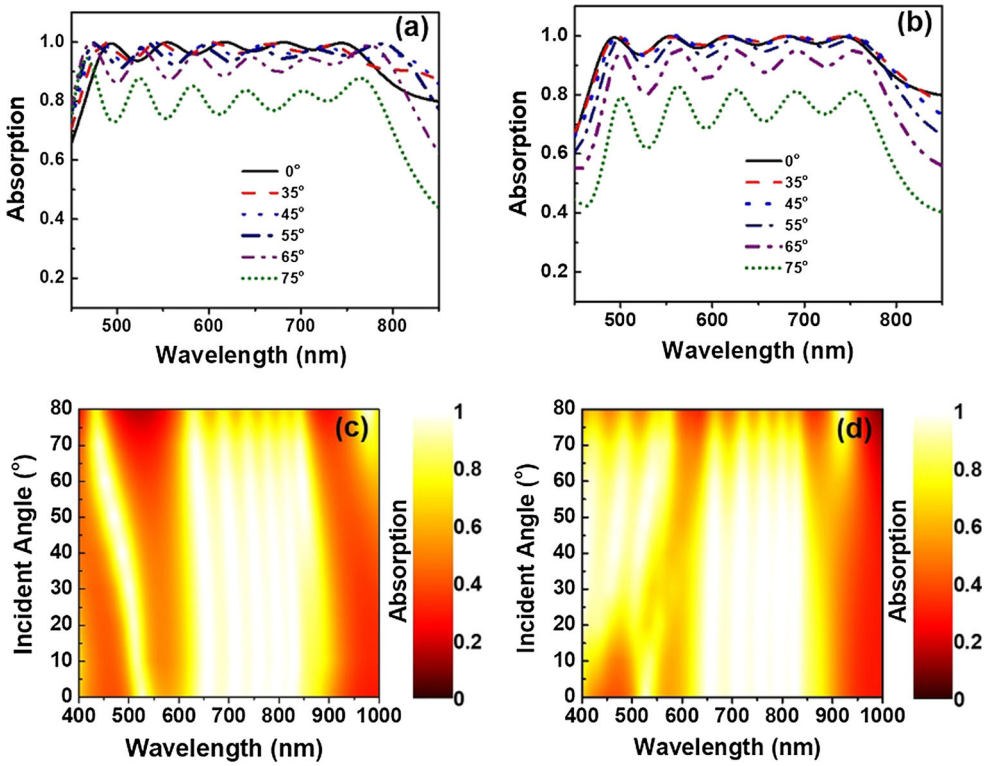

Fig. 5. Absorption efficiency as function of angle of incidence under (a, c) TE and (b, d) TM polarizations. (a) and (b) show the absorptivity at selected angles of incidence.

polarization angles. As expected, the absorptivity for different polarization angles remained absolutely unchanged for both TE and TM polarization when changing the polarization angle, indicating that the MA is insensitive to polarization angle. This insensitivity can be explained based on its symmetrical structure.

To investigate the absorption mechanism of the proposed MA, the distributions of induced magnetic field at three wavelengths of 475 nm, 570 nm, and 750 nm are shown in Fig. 7, for the MA designed with tilt angle of 88° and lattice constant of 150 nm. Figure 7 shows that EM waves in a specified waveband are concentrated in a certain part of the MA. With decreasing wavelength, the EM wave tends to accumulate at higher part; For example, EM energy at the shortest wavelength of 475 nm is absorbed at the top of the MA. This means that the resonance wavelength is directly proportional to the MA size.[10,18,19] It was reported that an individual single-layer MA structure exhibited a narrow perfect absorption peak due to magnetic resonance.[13,19]

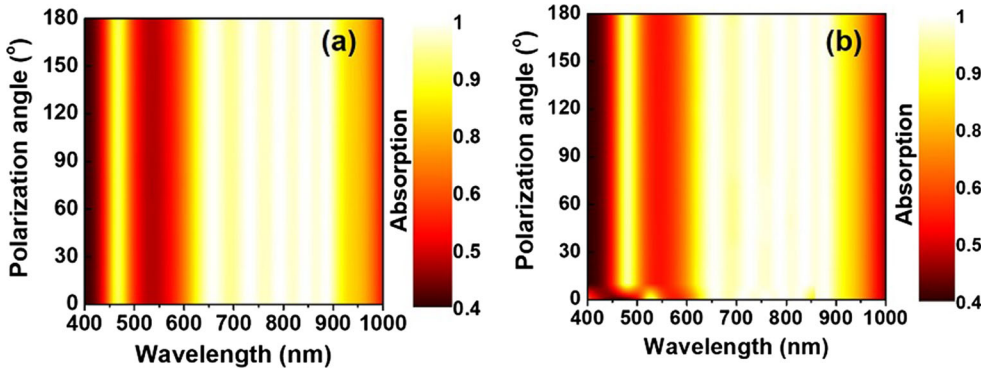

Fig. 6. Absorption spectra according to polarization angle for (a) TE and (b) TM polarizations at normal angle of incidence.

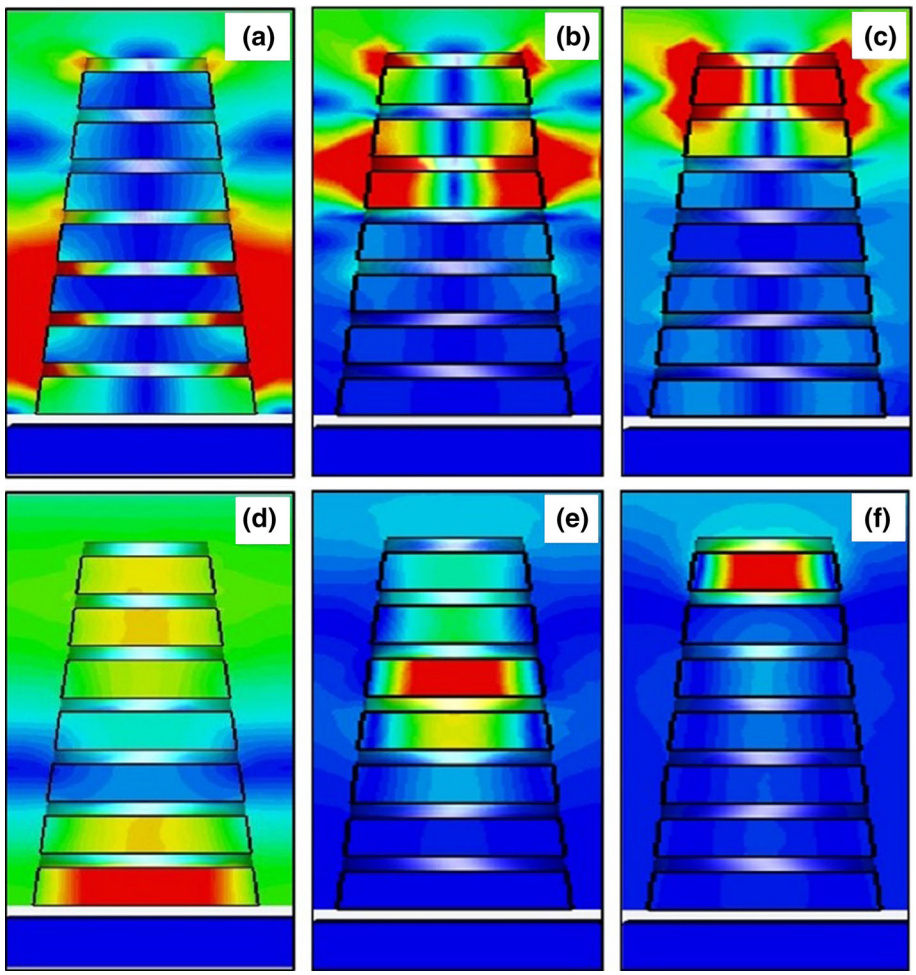

Fig. 7. Distribution of magnetic amplitude on central cross-section of unit cell of proposed MA for incident wavelength of (a) 750 nm, (b) 570 nm, and (c) 475 nm.

Therefore, broadband absorption can be observed when combining several continuous absorption peaks as the size of adjacent layers changes gradually based on the tailoring of the tilt angle. Moreover, the magnetic field is concentrated not only in the main resonant layer but also in adjacent layers. This confirms the existence of the interlayer exchange coupling effect between adjacent layers.[14,20,21] Such an exchange coupling effect can contribute significantly to obtaining high absorptivity

across an ultrabroadband range, though a considerable change in the absorptivity of single-layer MA structures with different disk sizes and fixed lattice constant was observed.[18,19]

CONCLUSIONS

An ultrabroadband MA in the visible region formed using a periodic array of metallic–dielectric multilayered conical frustums was studied numerically. The bandwidth and absorption properties were controlled by tailoring the tilt angle of the conical frustums and the lattice constant of the unit cell, having optimum values of 88° and 150 nm, respectively. The proposed MA shows absorptivity above 80% across a wide bandwidth from 474.4 nm to 784.4 nm, which is retained at large angles of incidence up to 65°. Furthermore, due to its rotationally symmetric structure in the E–H plane, the MA is insensitive to polarization angle for both TE and TM. Based on the obtained absorption results, the proposed MA has significant potential for applications in the visible region.

ACKNOWLEDGEMENTS

We acknowledge Prof. V. D. Lam from the Institute of Materials Science (IMS), Vietnam Academy Science and Technology (VAST), Vietnam for his help with simulations. This research is funded by Vietnam National Foundation for Science and Technology Development (NAFOSTED) under Grant Number 103.02-2017.367.

REFERENCES

1. J.B. Pendry, *Phys. Rev. Lett.* 85, 3966 (2000).
2. D. Schurig, J.J. Mock, B.J. Justice, S.A. Cummer, J.B. Pendry, A.F. Starr, and D.R. Smith, *Science* 314, 977 (2006).
3. N.I. Landy, S. Sajuyigbe, J.J. Mock, D.R. Smith, and W.J. Padilla, *Phys. Rev. Lett.* 100, 207402 (2008).
4. F.I. Baida, M. Boutria, R. Oussaid, and D. Van Labeke, *Phys. Rev. B* 84, 035107 (2011).
5. Y. Wang, T. Sun, T. Pauldel, Y. Zhang, Z. Ren, and K. Kempa, *Nano Lett.* 12, 440 (2012).
6. J. Fang, I. Levchenko, W. Yan, I. Aharonovich, M. Arameshi, S. Prawer, and K. Ostrikov, *Adv. Opt. Mater.* 3, 750–755 (2015).
7. F.B.P. Niesler, J.K. Gansel, S. Fischbach, and M. Wegener, *Appl. Phys. Lett.* 100, 203508 (2012).
8. B. Wang, K.H. Teo, T. Nishino, W. Yerazunis, J. Barnwell, and J. Zhang, *Appl. Phys. Lett.* 98, 254101 (2011).
9. N.T. Hien, B.S. Tung, N.T. Tuan, N.T. Tung, Y.P. Lee, N.M. An, and V.D. Lam, *Adv. Nat. Sci. Nanosci. Nanotechnol.* 5, 025013 (2014).
10. H. Wang and L. Wang, *Opt. Exp.* 21, 197523 (2013).
11. T.M. Cuong, N.T. Thuy, and L.A. Tuan, *J. Electron. Mater.* 45, 2591 (2016).
12. S. Liu, H. Chen, and T.J. Cui, *Appl. Phys. Lett.* 106, 151601 (2015).
13. H. Xiong, J.S. Hong, C.M. Luo, and L.L. Zhong, *J. Appl. Phys.* 114, 064109 (2013).
14. N.T.Q. Hoa, P.H. Lam, and P.D. Tung, *Microw. Opt. Technol. Lett.* 59, 1157 (2017).
15. Y. Cheng, B. HE, J. Zhao, and R. Gong, *J. Electron. Mater.* 46, 1293 (2017).
16. Y.J. Yoo, Y.H. Zheng, Y.J. Kim, J.Y. Rhee, J.H. Kang, K.W. Kim, H. Cheong, Y.H. Kim, and Y.P. Lee, *Appl. Phys. Lett.* 105, 041902 (2014).
17. F. Ding, Y. Cui, X. Ge, Y. Jin, and S. He, *Appl. Phys. Lett.* 100, 103506 (2012).
18. C.W. Cheng, M.N. Abbas, C.W. Chiu, K.T. Lai, M.H. Shih, and Y.C. Chang, *Opt. Express* 20, 10376 (2012).
19. D.T. Viet, N.T. Hien, P.V. Tuong, N.Q. Minh, P.T. Trang, L.N. Le, Y.P. Lee, and V.V. Lam, *Opt. Commun.* 322, 2019 (2014).
20. M. Lobet, L. Mercy, M. Sarrazin, O. Deparis, and L. Henrard, *Opt. Express* 22, 12678 (2014).
21. X.J. He, S.T. Yan, Q.X. Ma, Q.F. Zhang, P. Jia, F.M. Wu, and J.X. Jiang, *Opt. Commun.* 340, 44 (2015).